Available online at www.sciencedirect.com
ScienceDirect
Procedia Engineering 2 (2010) 1895–1903
Procedia Engineering
www.elsevier.com/locate/procedia

Fatigue 2010

Considerations about the welding repair effects on the structural integrity of an airframe critical to the flight-safety

Marcelino P. Nascimento[a]*, Herman J. C. Voorwald[b]

[a,b] *UNESP- Univ Estadual Paulista, Department of Materials and Technology – FEG/DMT, 333 Ariberto Pereira da Cunha Ave., Guaratinguetá/SP – CEP: 12516-410, Brazil*

Received 8 March 2010; revised 10 March 2010; accepted 15 March 2010

Abstract

Structures critical to the flight-safety are commonly submitted to several maintenance repairs at the welded joints in order to prolong the in-service life of aircrafts. The aim of this study is to analyze the effects of Tungsten Inert Gas (TIG) welding repair on the structural integrity of the AISI 4130 aeronautical steel by means of experimental fatigue crack growth tests in base-material, heat-affected zone (HAZ) and weld metal. The tests were performed on hot-rolled steel plate specimens, 0.89 mm thick, with load ratio R = 0.1, constant amplitude, at 10 Hz frequency and room temperature. Increase of the fracture resistance was observed in the weld metal but decreasing in the HAZ after repair. The results were associated to microhardness and microstructural changes with the welding sequence.

Keywords: AISI 4130 aeronautical steel; fatigue crack growth; TIG welding; welded joints; HAZ; aircraft motor-cradle

1. Introduction

Fatigue in aircrafts has been subject of extensive investigation since 1950's, after the accidents with the English model "Comet" [1]. Nowadays, many fractures of materials are still caused by fatigue as a consequence of either inadequate project or any notch produced during manufacturing and maintenance operations of aircrafts [2]. Maintenance operation errors specifically are responsible for serious safety problems and fatal accidents [3]. For this reason, the flight-safety has been the main concern of the aeronautical authorities all over the world.

Basically, the aeronautical projects should take into account the difficulties of transporting a load against the gravity force during take-off and flight, and discharge it in an efficient way, with minimum cost and maximum safety, because failures in any of these stages will implicate catastrophic accidents, involving human lives [4]. During flight an airplane is subjected to complex loads from varied frequency and magnitude as a result of abrupt maneuvers, wind bursts, motor vibration, helixes efforts and so forth. Consequently, an aircraft is a result of extensive researches and developments toward assure the continued airworthiness and increasing its in-service life.

For several aircraft models (e.g. agricultural, military training and acrobatic) the most solicited and repaired component is one that supports the motor, called "Motor-Cradle" (Fig. 1) [5].

* Corresponding author. Tel.: +55-12-3123-2853; fax: +55-12-3123-2852.
E-mail address: marcelino.nascimento@gmail.com

1877-7058 © 2010 Published by Elsevier Ltd.
doi:10.1016/j.proeng.2010.03.204

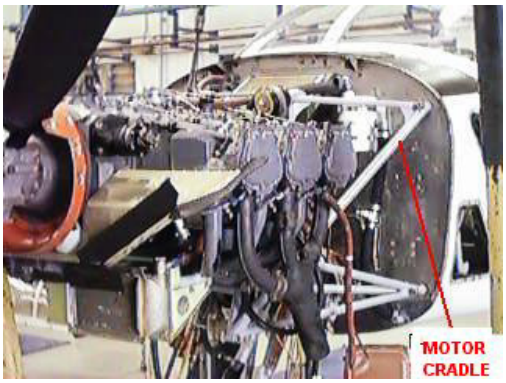

Fig. 1. Motor-cradle assembly in a T-25 Universal Brazilian aircraft.

This component presents a geometrically complex structure made from AISI 4130 tubular steel of different dimensions and TIG welded in several angles [5, 6]. For the Brazilian aircrafts T-25 Universal and T-27 Tucano, for example, besides supporting the motor in balance, the motor-cradle also maintains the nose landing gear fixed at the other extremity. Since the motor cradle is a component critical to the flight-safety, the aeronautic standards are extremely rigorous in its manufacturing, by imposing a "zero-defect index" on the final weld seam quality (Safe-Life philosophy), which is 100% inspected by non-destructive testing/NDT [5, 6]. For this reason, welded aeronautic structures are frequently subjected to successive repairs in accomplishment to current standards. As a consequence, components approved by NDT may contain a historic record of welding repairs whose effects on their structural integrity are not computed. In addition, these structures are also submitted to weld repairs along their operational life, turning this question more complex. An investigation on 157 motor-cradles fracture reports of the T25-Universal aircraft model indicates that all of them occurred at welded joints as a result of fatigue cracks, reducing the “Time-Before-Fail” from 4.000 h to 50 h of flight [5]. Motivated by high fracture incidence of this particular component, an extensive research program to evaluate the manufacturing and maintenance weld repair effects on the structural integrity, mechanical properties and microstructural changes has been conducted [6]. The aim of this study is to analyze the effects of the TIG welding repair on the structural integrity of the AISI 4130 aeronautical steel by means of experimental fatigue crack growth tests in base material (BM), heat affected zone (HAZ) and weld metal (WM).

2. Experimental Procedure

For the present research-work flat welded specimens from hot-rolled AISI 4130 aeronautic steel, 0.89 mm thick, were used. The chemical compositions (wt%) from the base material and filler metal are presented in Table 1 (Fe in balance).

Table 1. Chemical compositions

Composition (wt%)	C	Mn	P_{MAX}	S_{MAX}	Si	Mo	Cr	Cu
Specified BM (*)	0.28-0.33	0.40-0.60	0.035	0.040	0.15-0.30	0.15-0.25	0.80-1.10	0.10
Specified WM (**)	0.28-0.33	0.40-0.60	0.008	0.008	0.15-0.35	0.15-0.25	0.80-1.10	0.10
Filler metal	0.30	0.50	0.004	0.003	0.25	0.18	0.91	0.042
Plate 0.89 mm thick	0.32	0.57	0.013	0.008	0.28	0.18	0.90	0.01

** AMS 6457 B – Turballoy 4130 Steel.*

*** AMS T 6736 A (2003) – for chromium-molybdenum (4130) seamless and welded steel tubing of aircraft quality.*

The mechanical properties obtained from smooth flat samples and originally welded specimens (OR) -- with central weld seam crossed to the hot-rolled plate direction --, are indicated in Table 2. The hot-rolled plates presented 65 HR_A in the “as-received” condition. The monotonic tensile tests were performed in accordance with

ASTM E 8M by means of a servo-hydraulic INSTRON test machine, applying 0.5 mm/min displacement rate and a preload equal to 0.1 kN.

Table 2: Mechanical properties obtained from the welded and non-welded specimens.

Specimens	Yielding (0.2% offset)	Ultimate strength	Ruptura stress	Elongation (25mm length)	Yielding/ultimate strength ratio
Base-metal	740 ± 2	809 ± 3	669 ± 11	8.48 ± 1.00	0.91 ± 0.00
Welded	671 ± 20	778 ± 17	643 ± 26	3.81 ± 0.26	0.86 ± 0.01

2.1. Welding and Re-welding Procedures

The most commonly employed welding process for manufacturing aeronautical structures is Tungsten Inert Gas (TIG), or Gas-Tungsten Arc-Welding (GTAW), which is appropriate to weld thin thickness materials and to allow the necessary variable control, resulting in high-quality and defect-free weld beads. The TIG welding process was carried out in accordance with the Brazilian Aeronautic Standard EMBRAER NE 40-056 TYPE 1 (for components critical to the flight-safety), with a protective 99.95% purity argon-gas and filler metal AMS 6457 B – Turballoy 4130. A Square Wave TIG 355/Lincoln equipment was manually employed by an expert aeronautic welder. All the welding parameters were controlled, and the main ones are indicated in Table 3. Also, all the welded joints were subjected to X-ray non-destructive analysis by the Brazilian Aerospace Technical Centre (CTA/IFI), which proved the acceptable quality of the welds according to MIL-STD-453, EMBRAER - NE-57-002 and ASTM E-390 standards.

Table 3. Principal TIG welding parameters.

Direct current	DCEN
Welding position	Flat
Welding voltage	12 V
Welding current	40 A
Welding speed	18.0 cm.min^{-1}
Flow rate	5 L.min^{-1}
Pre heating	None
Heat-input	1.50 kJ.cm^{-1}
Filler metal diameter	1.6 mm

The welding direction was always perpendicular to the hot-rolling process (direction) of the plate. Before welding, samples were cleaned with chlorinated solvent to oxide removal and fixed on a backing bar to avoid contamination and porosity in the weld root. After the welding/re-welding process neither subsequent heat treatment to residual stresses relief nor subsequent removal of the weld bead was carried out, in order to simulate the real condition of the original aeronautic structure. Due to the plate thickness, only one weld single-pass was required. The weld repair was carried out by overlapping that previous weld seam. Fig. 2 schematically illustrates the weld repair process by overlapping, which it is usually applied on welded structures along their in-service life of aircrafts (maintenance welding). The heat-input applied was kept constant for all the welded and re-welded specimens.

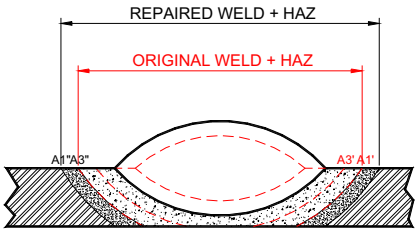

Fig. 2. Weld repair process by overlapping.

2.2. Fatigue Crack Growth Tests

For the fatigue crack growth tests, specimens were prepared according to ASTM E 647, following the LT directions (Fig. 3) The tests were performed on a servo-hydraulic machine upon a sinusoidal load, at room temperature, constant amplitude, load ratio R = 0,1 and at 10 Hz frequency. The specimens were subdivided in three groups:

- GROUP I: specimens of base-material with central cracks, M(T);
- GROUP II: welded specimens with central cracks, M(T), which were located in the weld metal (WM);
- GROUP III: specimens with central cracks, M(T), which were located in the HAZ.

The central notch, necessary to generate the fatigue pre-cracks, was performed in accordance to ASTM E 647, by electric discharge machine (EDM). The maximum stress applied was 200 MPa, approximately, for all specimens.

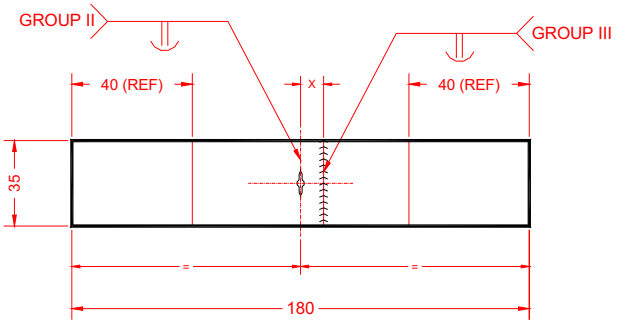

Fig.3. M(T) specimen configuration for fatigue crack growth tests

2.3. Microstructural and Microhardness Analyses

For microstructural analysis a chemical etching Nital 2% was applied for 5s. Vickers microhardness measurements were obtained at 0.0254 mm intervals throughout the regions under analysis (base-material, HAZ sub-regions and weld metal), applying a 1 N load.

3. Results and Discussion

Figs. 4(a) and (b) present the *a x N* curves of all conditions mentioned. First of all, from Fig. 4(a) one can see that the fatigue crack grew faster in the original WM, followed by the BM and repaired WM, respectively. However, from Fig. 4(b), the fatigue crack grew faster in HAZ (from the original and repaired WM) than BM.

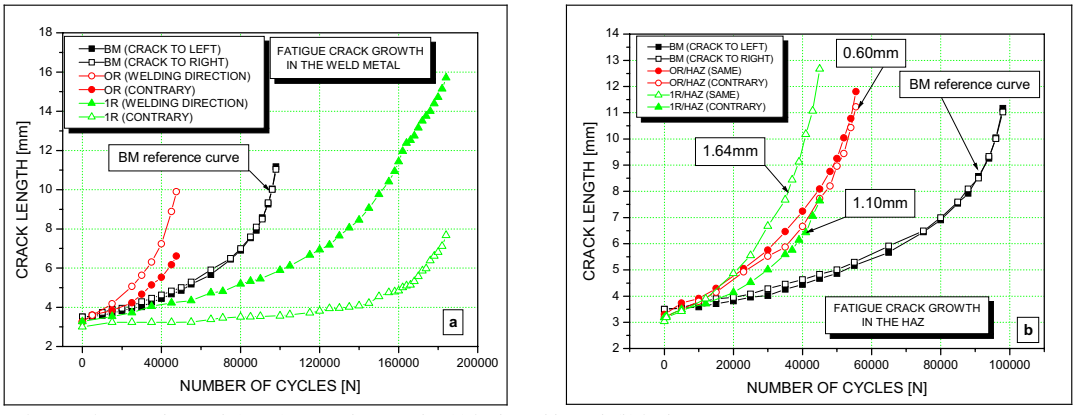

Fig. 4. Fatigue crack growth (a x N) curves from cracks: (a) in the weld metal; (b) in the HAZ.

Unlike as in the material-base, where both left and right cracks grew in a symmetrical way as a function of the microstrutural homogeneity, in WM and HAZ both left and right cracks grew asymmetrically. For the WM, in addition to the microstrutural heterogeneity, this is due to the solidification process of the weld pool, whose columnar grains follow the weld direction (weld travelling). So, the nucleation and growth of the columnar grains begins from the base-material at the weld joint (fusion line) into the central area of the weld seam (center-line), where they do give arise a preferential road for the fast propagation of cracks. Contrary to the weld travelling, on the other hand, it is observed that the crack spread very slowly. These behaviours are strictly related to the heat-input employee and represent a potential defect in weld seams. For HAZ, however, it is probable that the effect of the welding direction is not so effective. From Fig. 4(b) it is observed that the cracks nucleating and grew in different sub-regions of the HAZ, as indicated by distance values faraway of the fusion-line, inside box. That is, it is possible that the crack has traveled other sub-regions of the HAZ, with different textures, hardness and microstruture, along its path. Consequently, the necessary periodic inspections at the welded joints, based in the Damage Tolerance and Flaw-Safe philosophies, should take into account the asymmetric fatigue crack growth presented.

Figs. 5(a) and (b) present the *da/dN x* ΔK curves of all conditions tested. Due to asymmetric fatigue crack propagation in both WM and HAZ, for the configuration of the referred curves just that faster crack was considered. Fig. 5(a) reveals that the originally welded specimen has a faster *da/dN* than all the other conditions. On the other hand, it is also clear that the weld repair effectively retarded the crack propagation into the weld metal. For the BM (AISI 4130 steel, 0.89 mm thick), it is possible to observe that stress intensity factor threshold (ΔK_{th}) is around 20 MPa.m$^{1/2}$ and the toughness value in state of plane stress achieved 45 MPa.m$^{1/2}$. For original WM the toughness value in state of plane stress achieved 48 MPa.m$^{1/2}$, and for repaired WM the toughness value in state of plane stress achieved 44 MPa.m$^{1/2}$. Yet, for the repaired WM, it is also possible to esteem that stress intensity factor threshold (ΔK_{th}) is around 10 MPa.m$^{1/2}$.

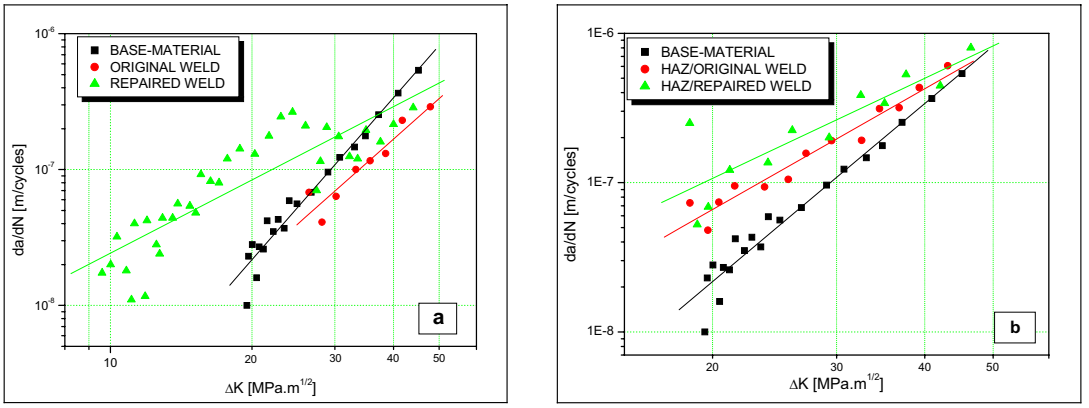

Fig. 5. da/dN vs. ΔK curves for fatigue crack growth in: (a) original and repaired weld metal; (b) original and repaired HAZ.

In addition, it is interesting to pay attention to the great irregularity of the crack growth rate (dispersion of the points in the curve) in the repaired WM, which can be attributed to the crack closing during its propagation.

On the other hand, Fig. 5(b) reveals that the original and repaired HAZ specimens presented a faster da/dN than the base-material. However, it is also clear that the welding repair effectively retarded the crack propagation along the new HAZ. For original HAZ the toughness value in state of plane stress achieved 43 MPa.m$^{1/2}$, and for repaired HAZ the toughness value in state of plane stress achieved 46.5 MPa.m$^{1/2}$. Yet, the little irregularity of the crack path is also due to different textures, hardness and microstrutures which it traveled in other sub-regions of the HAZ. The fatigue crack behaviors presented in Figs. 4 and 5 are also related to very low elongation value (3.81% average) obtained from the monotonic tension tests aforementioned.

Based on the presented curves the "*C*" and "*n*" constants were determined for the three mentioned areas (base material, HAZ and weld metal) by using the Paris and Erdogan' equation [7], described ahead. The values obtained are presented in Table 4.

$$\frac{da}{dN} = C(\Delta K)^n \quad (1)$$

where:
$da/dN \rightarrow$ fatigue crack propagation rate;
C e $n \rightarrow$ constant of the material;
$\Delta K \rightarrow$ stress intensity factor variation.

Table 4. *C* and *n* values obtained from the Fig. 5.

Group	C	n	R
Base-Material	1.52E-13	3.96	0.97
Original Weld	2.02E-12	3.07	0.95
HAZ of Original Weld	2.10E-11	2.68	0.97
Repaired Weld	3.92E-10	1.79	0.86
HAZ of the Repaired Weld	1.33E-10	2.23	0.87

Fig. 6 presents the microhardness profile in both original and repaired welded joints.

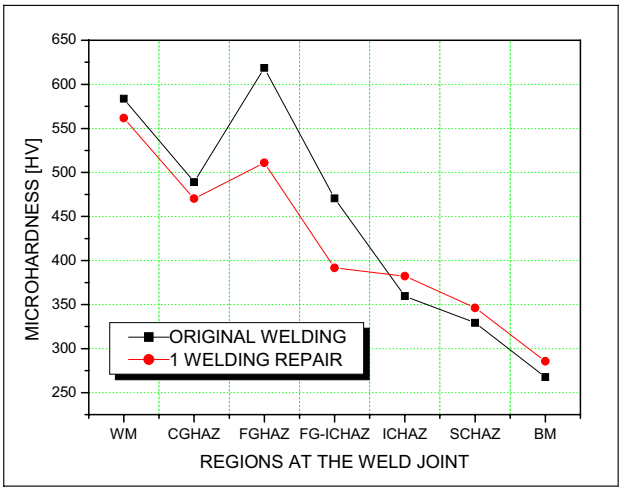

Fig. 6. Microhardness profile from the weld metal, through HAZ regions to base-material.

From Fig. 6 one can observe that both curves presented similar tendency along HAZ sub-regions, i.e.: reduction of the microhardness values from FGHAZ (Fine-Grain HAZ) to BM (naturally); high microhardness values for WM, which decrease in the CGHAZ and increase again in the FGHAZ, as a consequence of TIG welding and re-welding process (high cooling speed associate to the low heat-input applied). Also, the microhardness values presented are totally coherent, i.e.: the lower hardness, the higher grain size (CGHAZ). For the weld metal (WM), CGHAZ and FGHAZ regions, all the microhardness values decreased with the weld repair application, which implicates a consequent increasing of the respective grain-sizes (lower cooling speed). Since the heat-input was kept constant for both original and repaired welding, the uneven microhardness values verified in the weld metal (WM) were due to the weld repair process by overlapping the prior weld seam, resulting in larger weld metal volume, which differently affected the cooling speed in that region (lower cooling rate/higher grain size). With respect to

fatigue crack growth curves (Figs 4 and 5), it is well known that the crack propagate faster in harder material due to smaller plastic zone at the crack tip.

These results are also related to microstructural changes observed in the three analyzed areas. Figs. 7 and 8 present the microstructures at the welded joints.

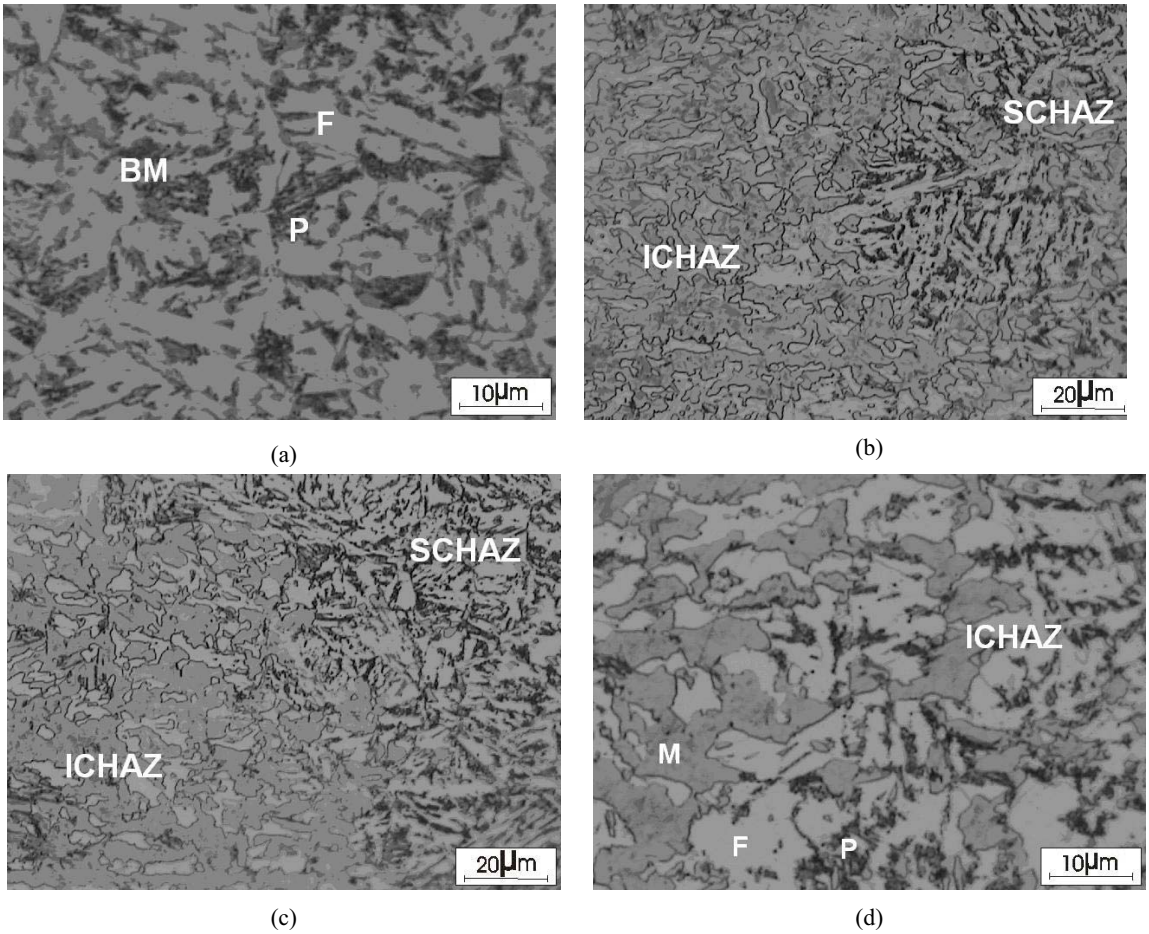

Fig. 7: Base-material and base-material/HAZ transition microstructures (typical): (a) Base-material; (b) SCHAZ-ICHAZ of the original weld; (c) SCHAZ-ICHAZ of the welding repair; (d) ICHAZ of the welding repair. F=Ferrite; P=Perlite; M=Martensite. Nital 2%.

Fig. 7(a) shows the normal products of transformation from austenite, i.e. ferrite and perlite. So, the fatigue crack will find larger resistance to propagate through the ferrite and perlite grains due to the microstructural barriers offered, associated to lower hardness values aforementioned.

From Fig. 7(b–d) the beginning of the transformation from perlite to austenite is observed (to martensite, upon subsequent cooling) along the SCHAZ/ICHAZ regions.

Fig. 8 presents microstructures of the weld metal (original and repaired) and respective CGHAZ, both basically constituted by martensite, which is a very hard and fragile microstructure. As aforementioned, the higher the hardness the faster the fatigue crack propagation. The microstructural effect on the fatigue crack growth for varied steels has been reported by several investigators [9], who concluded that tempered martensite has a higher resistance

to the crack propagation. Thus, it is possible that the welding repair was able to temper the original martensite structure and consequently decreasing the fatigue crack propagation in the weld metal and HAZ.

Yet, from Fig. 8(d), one can observe the presence of aligned second phase ferrite (FS(A)) in the repaired WM. It is well known that this constituent can delay the fatigue crack propagation by altering its path.

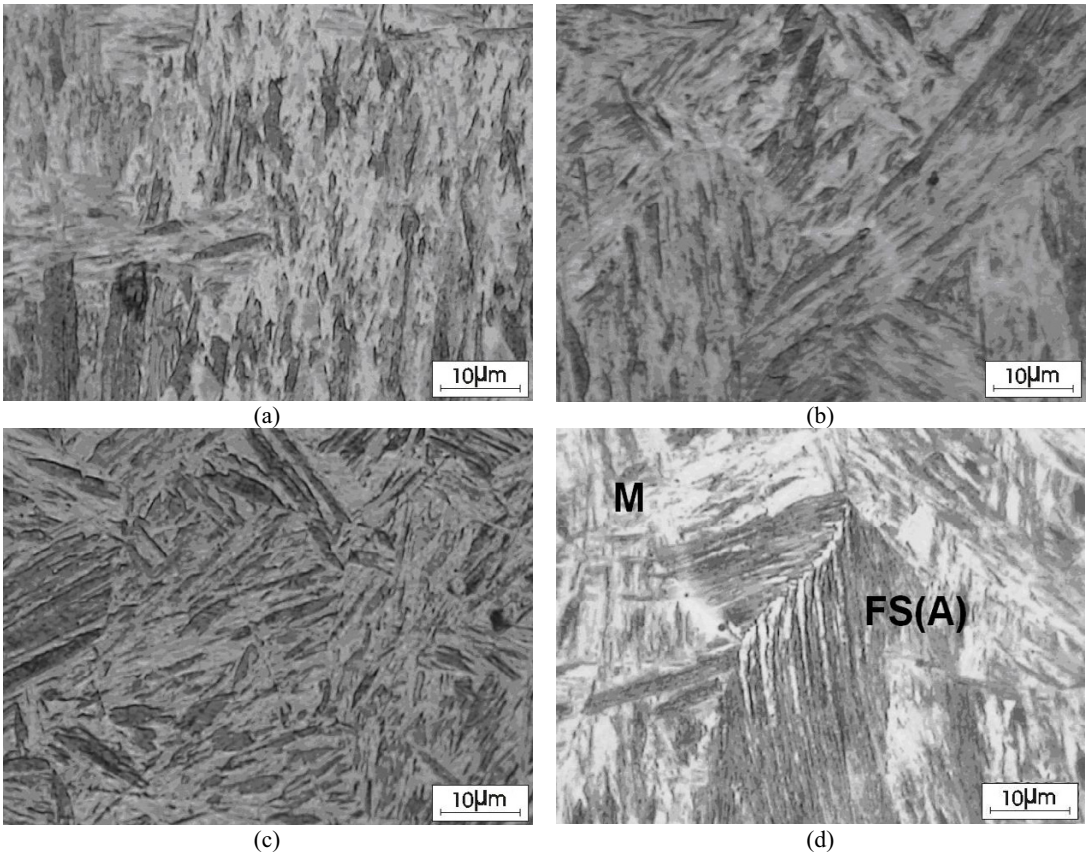

Fig. 8. Microscopic analysis of the weld metal and CGHAZ: (a) Original CGHAZ; (b) Original Weld Metal; (c) CGHAZ from the repaired weld; (d) Weld Metal from the repaired weld. Nital 2%.

4. Conclusions

In the present paper the following conclusions may be drawn:

1. The TIG welding process reduced the ultimate tensile strength, as well as the yielding tensile strength and the ductility of the AISI 4130 steel.
2. Fatigue crack in original weld metal grew faster in relation to HAZ and base material.
3. The base-material presented larger resistance to fatigue crack propagation. This behavior was associated to lower microhardness values and microstructure constituted by fine perlite-ferrite grains.
4. The TIG welding travel direction affected the fatigue crack propagation and consequently the fracture resistance or fracture toughness of the AISI 4130 steel for the applied heat-input.
5. TIG welding repair process induced microstructural and microhardness changes on the weld metal and improved its strength to the crack propagation.

Acknowledgements

The authors are grateful to FAPESP/processes No. 99/11948-6 and 08/56424-5.

References

[1]. Payne, A. O. The fatigue of aircraft structures, Engineering Fracture Mechanics *Engineering Fracture Mechanics* 1976, **8**, 157-203.

[2]. Goranson, U. G. Fatigue issues in aircraft maintenance and repairs *International Journal of Fatigue* 1993, **19**, S3-S21.

[3]. Latorella, K. A. and Prabhu, P. A review of human error in aviation maintenance and inspection, International Journal of Industrial Ergonomics V. *International Journal of Industrial Ergonomics* 2000, **26**, 133-161.

[4]. Godefroid, L. B. Fatigue crack growth under constant and variable amplitude loading in aluminium alloys of aeronautical applications, Ph.D. Thesis, COPPE, Federal University of Rio de Janeiro 1993, Brazil.

[5]. Nascimento, M.P., Voorwald H. J. C. An evaluation on the fatigue crack growth in re-welded AISI 4130 aeronautical steel, in: *Eighth International Fatigue Congress/FATIGUE 2002. Stockholm-Sweden* 2000, **5** 3463-3472.

[6]. Nascimento, M.P. Effects of TIG welding repair on the structural integrity of AISI 4130 aeronautical steel. Ph.D Thesis in Mechanical Engineering. State University of São Paulo/UNESP-FEG, Brazil (in Portuguese), 2004, 240p.

[7]. Wei, M.Y. and Chen, C. Fatigue crack growth characteristics of laser-hardened 4130 steel *Scripta Metallurgica et Materialia* 1994, **31**, 1393-1398.

[8]. Paris, P. and Erdogan, F. A Critical Analysis of Crack Propagation Laws *Journal of Basic Engineering, Transactions of the ASME* 1963, **85**, 528-534.

[9]. Chiarelli, M., Lanciotti, A. and Sacchi, M. Fatigue resistance of MAG welded steel elements *International Journal of Fatigue* 1999, **1**, 1099-110.